Geothermics 56 (2015) 1–16

Contents lists available at ScienceDirect

Geothermics

journal homepage: www.elsevier.com/locate/geothermics

Data integration and favourability maps for exploring geothermal systems in Sicily, southern Italy

Eugenio Trumpy*, Assunta Donato, Giovanni Gianelli, Gianluca Gola, Angelo Minissale, Domenico Montanari, Alessandro Santilano, Adele Manzella

Institute for Geosciences and Earth Resources, National Research Council of Italy, Via Moruzzi 1–56124, Pisa, Italy

ARTICLE INFO

Article history:
Received 31 May 2014
Accepted 3 March 2015
Available online 25 March 2015

Keywords:
Sicily
Geothermal energy
GIS model
Favourability map

ABSTRACT

This paper describes a data integration tool used to identify potentially undiscovered geothermal resources in the island of Sicily. The factors facilitating the recovery of exploitable geothermal energy were defined, and their spatial correlation established by Geographic Information System (GIS) models.

By prioritizing favourable conditions using an Index Overly method, "favourability" maps of Sicily were obtained. The maps considered both geological and economic aspects, and energy recovery was considered for current technologies. Our approach and maps are useful for developing and planning local or national energy policies including geothermal energy.

1. Introduction

Italy is a geothermal country: the fifth geothermal power producer in the world (Bertani, 2012), the first to produce geothermal electricity at an industrial scale, and a high exploiter of geothermal heat. Geothermal energy provides a significant contribution to renewable energy sources (RES) in Italy; however its future potential still needs to be fully assessed. Along with its high potential, geothermal energy is ideally suited to baseload operations which intermittent resources are unable to provide on an economic basis.

Geothermal energy is seldom considered in energy planning at national and regional levels in Italy and, due to relative lack of specific incentives and rather difficult and lengthy regulations. New geothermal projects, both for demonstration and research, are very difficult to establish in Italy. A fundamental aspect of any energy policy is the certainty around assessment of the nation's natural energy resources, including geothermal. Therefore, a key requirement for further exploiting geothermal energy by increasing the number of projects as well as the variety of uses is to clearly identify and rank resources and opportunities.

This paper provides a practical analytical framework for the systematic capture of information relevant to the assessment of geothermal resources of Sicily, one of the largest islands of southern Italy.

Geothermal assessments follow a broad search for the existing data provided by a number of sources. In Italy, the most relevant existing information regarding geothermal resources includes deep temperature data from oil and gas exploration boreholes as well as physical and chemical information from wells and natural thermal springs.

Data analysed in this study includes geothermal data gathered in the 1980s from an inventory of geothermal resources in Italy (ENEL et al., 1988), which are organized in the National Geothermal Database, and managed by the Italian National Research Council. The database was then complemented with hydrocarbon well the Italian Ministry of Economic Development. In spite of data improvements, information remains unevenly distributed and only covering a small area of Italy. In areas lacking boreholes and thermal springs, other indirect information can be taken into account from geological/volcanological, geochemical and geophysical surveys in order to assess and rank the geothermal potential of areas of interest. This useful, but scattered information regarding underground conditions was retrieved from public reports, scientific papers, and other databases established for various uses.

The approach described here and applied to Sicily is aimed at organizing and integrating subsurface data, and at providing a methodology to establish a hierarchy of geothermal areas based on their potential for conventional power production, where conventional refers to exploitation of moderate to high-enthalpy geothermal resources with natural permeability as opposed to enhanced geothermal systems (EGS). We introduce here the terminology of "favourability" maps, previously adopted by

* Corresponding author. Tel.: +39 050 315 2324; fax: +39 050 315 2323.
E-mail address: e.trumpy@igg.cnr.it (E. Trumpy).

http://dx.doi.org/10.1016/j.geothermics.2015.03.004
0375-6505/

similar studies (e.g., Prol-Ledesma, 2000; Coolbaugh et al., 2002; Noorollahi et al., 2007; Yousefi et al., 2010; Tufekci et al., 2010).

By upgrading and updating the last geothermal ranking for Sicily carried out at a national scale in the 1980s (ENEL et al., 1988; Cataldi et al., 1995), we believe that our work is important for the exploration of potentially concealed geothermal resources. Besides mapping known geothermal systems and contributing to reduced exploration risk, we have made the first step towards a more detailed and systematic resource reporting system in Italy. A reporting method is the basis for the portfolio management of geothermal resources and the selection of specific locations for geothermal power production projects.

In this paper we describe our approach, discuss the information used and provide the results obtained in mainland Sicily. Small volcanic islands of Sicily and their geothermal systems are not taken into account in this paper.

2. Data integration for mapping favourable geothermal areas and space data model tools

Geographical Information System (GIS) software provides tools for the spatial analysis of multiple parameters to assist selection of prospective sites, based on pre-defined criteria which we discuss in this paper. The approach of GIS-assisted management of information for exploration purposes has been successfully applied in other fields including regional mineral exploration (Bonham-Carter et al., 1988; Bonham-Carter et al., 1994; Bonham-Carter, 1991; Agterberg, 1989; Katz, 1991; Chung et al., 1992).

In applying GIS tools, the conceptual model plays an important role in the choice of layers that will be involved in making a favourability map, as well as for scoring and weighting the selected layers. The score and weight in each layer are assigned using statistical criteria or estimated on the basis of expert opinion, referred to as "data-driven" or "knowledge-driven" models respectively. In data driven modelling, the layers are combined using approaches such as logistic regression or weight of evidence, while knowledge-driven models usually employ Boolean operators, Index Overlay (IO) and Fuzzy Logic GIS methods (Bonham-Carter et al., 1994).

GIS is often used to define the spatial associations between different thematic information in a specific area in order to define suitable geothermal areas (Prol-Ledesma, 2000; Coolbaugh et al., 2002; Coolbaugh et al., 2005; Noorollahi et al., 2007; Noorollahi et al., 2008; Yousefi et al., 2007; Tufekci et al., 2010 and references therein).

Prol-Ledesma (2000) proposed an evaluation of the results using three different GIS knowledge driven models for siting geothermal wells, for planning further detailed explorations, and for expanding the boundaries of the known field being exploited. Coolbaugh et al. (2002), Coolbaugh and Shevenell (2004) characterised the most suitable locations for geothermal exploration in the Basin and Range province (Nevada, USA), involving GIS spatial analysis for integrating input maps and using a logistic-regression method. Noorollahi et al. (2007, 2008) dealt with GIS knowledge-driven models as a decision-making tool for geothermal exploration and well siting.

Yousefi et al. (2007) produced an assessment of promising geothermal areas in Iran, using logic operator integration methods to combine the input maps. EBA Engineer Consultants Ltd. (2010) produced geothermal favourability maps in the North West Territory of Canada for areas with and without geothermal gradient data. Potential areas in Anatolia (Turkey) have been identified by Tufekci et al. (2010) with a data-driven approach, using both "Index Overlay" and "Weight of Evidence" methods, as well as training points to obtain maps. In this study, these procedures were adapted to account for the specific geological context of Sicily.

To produce favourability maps for conventional geothermal systems in Sicily, we used a GIS model to combine geological, geophysical and geochemical evidence. Although much hydrocarbon well data were taken into account, only a small amount of direct geothermal information, such as geothermal wells and exploitation data, are available in Sicily. We therefore applied a knowledge driven model using, for our knowledge-driven GIS model, the Index Overlay (IO) method, which provides a flexible way to apply a common scale of values, to non-uniform inputs, thus creating an integrated analysis. When information is organized in thematic maps (e.g., raster layers) with diverse value scales and importance, the values can be classified and scored before being overlaid. In addition, each information layer receives a defined weight.

The average score of the resulting map is therefore:

$$\bar{S} = \frac{\sum_{i=1}^{n} S_{ij}}{\sum_{i=1}^{n} W_i} \quad (1)$$

where, S is the weighted score for each pixel, W_i is the weight for the ith thematic map, and S_{ij} is the score for the jth class of the ith thematic map (Bonham-Carter, 1994).

We used the raster calculator to perform a favourability analysis and to develop an integration model making use of the spatial analysis capabilities of the open source software Quantum GIS and GRASS GIS. These tools overlay raster elements using a common spatial resolution, a common origin for the coordinates, and the same number of cells.

3. Geological setting and thermal features of Sicily

Sicily is situated in a complex geodynamic setting of economic interest due to the occurrence of hydrocarbon, sulphur and salt ore deposits. Sicily is a sector of the south verging Apennine-Maghrebian orogenic belt, stacked since Late Oligocene and located along the African-European plate boundary. The "collisional" complex of Sicily (Catalano and D'Argenio, 1982; Catalano, 2004; Roure et al., 1990; Nigro and Renda, 1999; Bello et al., 2000; Monaco and De Guidi, 2006; Accaino et al., 2011) (Fig. 1), is made up of: (i) the "Foreland", cropping out in south-eastern Sicily (Hyblean carbonate platform) and located in the Sicily Channel, (ii) a narrow northwest dipping "Foredeep" and (iii) the "Chain", a complex fold and thrust belt locally more than 20 km thick (Catalano, 2013; Catalano et al., 2013)consisting, from internal to external, of a "European" element (Peloritani Units), a "Tethyan" element (Sicilide Units) and an African element (Maghrebian–Apenninic Units). Peloritani units, part of the European crystalline basement, constitute the northeastern corner of Sicily (Roure et al., 1990).

According to Catalano et al. (2002) and Catalano (2004), the central-western areas of Sicily are made up of an imbricated wedge of Meso-Cenozoic carbonate and siliciclastic rocks resulting from the deformation of different paleo-geographic domains. The tectonic edifice is made up mainly of an 8–9 km thick wedge of Meso-Cenozoic imbricated carbonate platforms (Panormide, Trapanese and Saccense Units). The intermediate structural level consists of a 2–3 km tectonic stack of basinal carbonate thrust sheets (Imerese and Sicanian). These are overlaid by the Oligo-Miocene siliciclastic deposits of the Numidian Basin (Giunta, 1985) and by remnants of the Mesozoic-Tertiary basinal deposits of Sicilide nappe. Neogene-Quaternary syn- and post-tectonic deposits overlay the "collisional" complex.

Active tectonic processes (Monaco et al., 1996; Corti et al., 2006; Visini et al., 2010; Doglioni et al., 2012), have given rise to several geothermal anomalies in this Mediterranean area. The heat

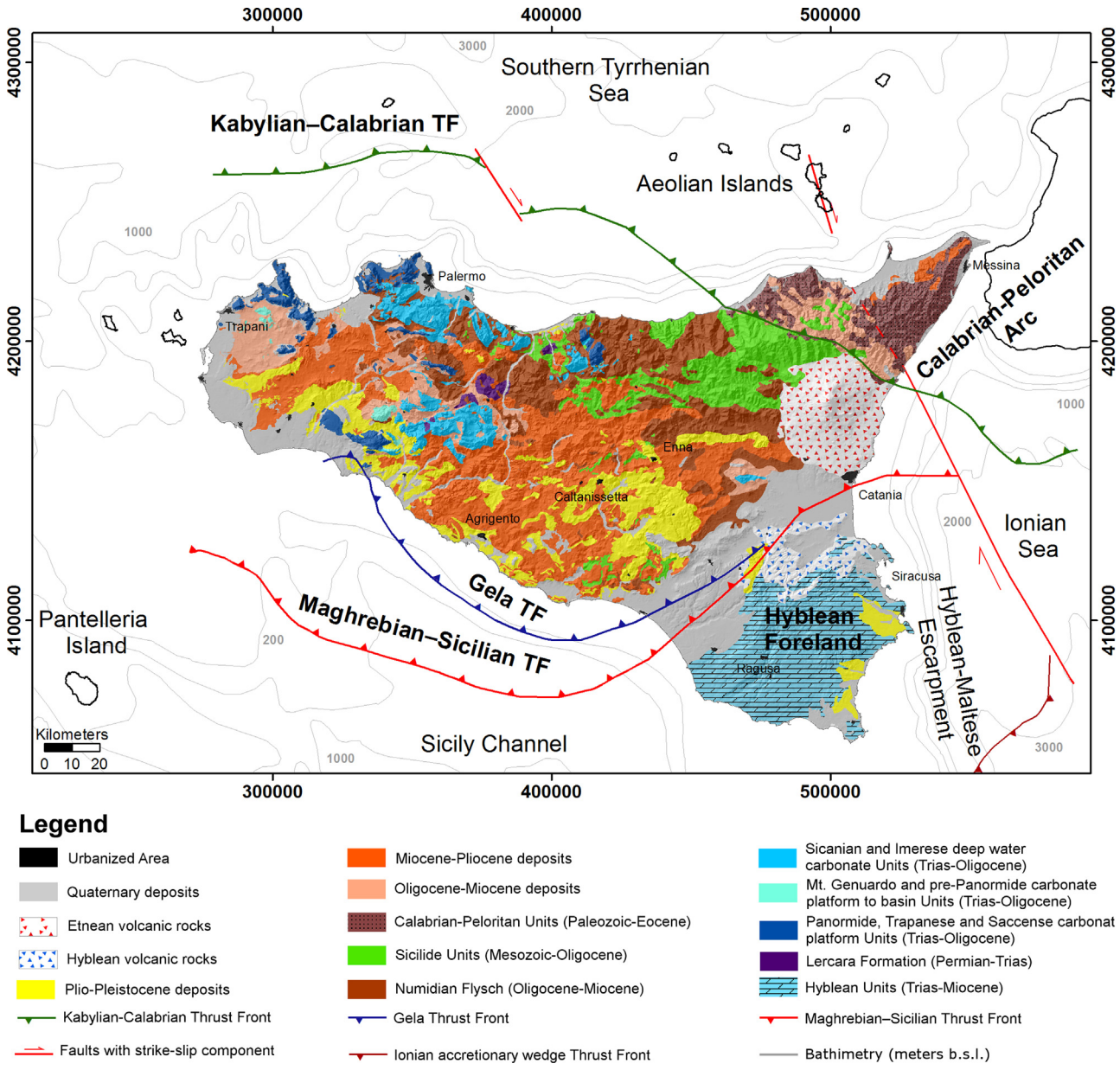

Fig. 1. Structural sketch map of Sicily (modified from Accaino et al., 2011).

flow density map as reported by Della Vedova et al. (2001), shows heat flux anomalies across: (i) the southern Tyrrhenian back-arc basin (more than 250 mW/m^2) characterized by a thinned crust with a Moho depth locally less than 10 km (Sartori, 2003), (ii) in the Aeolian Islands (200 mW/m^2) volcanic arc (Keller, 1982) and (iii) across the Sicily Channel rift (Corti et al., 2006) with values up to 460 mW/m^2 in the Pantelleria volcanic island.

Considering an average continental heat flow ranging from 57 mW/m^2 to 70 mW/m^2 (Sclater et al., 1980; Pollack et al., 1993; Davies and Davies, 2010), in the Sicilian mainland the heat flow density shows some anomalies (up to 90 mW/m^2) located in eastern Sicily (south of Mt. Etna) and in south-west Sicily, while low values occurred across the outcrops of Mesozoic carbonate probably due to infiltration of meteoric waters (Fig. 2) as previously suggested by Della Vedova et al. (2001).

There are several thermal manifestations in Sicily (Favara et al., 2001; Carapezza et al., 1977; Grassa et al., 2006) many of which are located in western Sicily, often near the outcrops of the Mesozoic carbonate units (Fig. 2), with temperatures up to 56 °C. Fumaroles and CO_2 rich emissions occur around Mt. Etna and the Hyblean Mts. (eastern Sicily).

4. Data sources

4.1. Geological data

The depth of potential geothermal reservoirs is one of the geological elements to input into the computation of geothermal favourability maps at a regional scale, with favourability decreasing with increasing depth of the top of these geothermal reservoirs. As reported by Montanari et al. (2013), the geophysical log information from exploratory oil and gas wells of Sicily combined with hydro-geochemical data suggest a hydraulic continuity among the distinct imbricate carbonate platforms hosting medium enthalpy geothermal fluids. Mesozoic limestone and dolostone units consequently act as a relatively continuous regional geothermal reservoir (Montanari et al., 2014) and all the geological units overlying the reservoir act as an impervious cover.

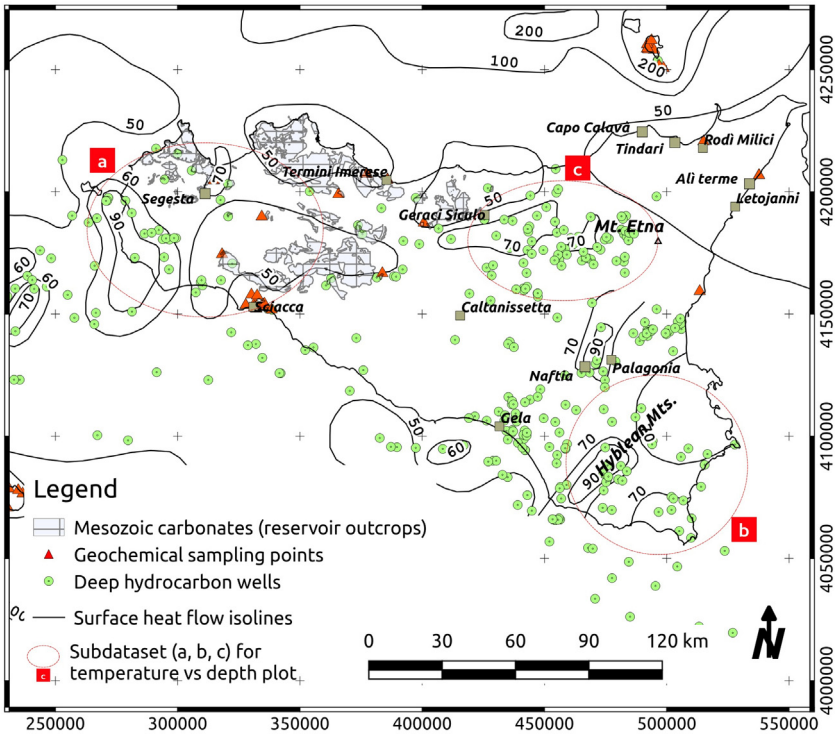

Fig. 2. Sketch map of source of data. Geochemical sampling points and deep wells are displayed as well as the heat flow density isolines (from Della Vedova et al., 2001). The outcrops of Mesozoic carbonate rocks, hosting the regional geothermal reservoir, are shown. Red boundaries limit the sectors (a, b, c) for which we display the temperature profiles in Fig. 3. (For interpretation of the references to colour in this figure legend, the reader is referred to the web version of this article.)

Existing geological and geophysical data combined with new data acquired in particular key areas, provided the input for a 3D geological model used to predict the top of the regional geothermal reservoir (Montanari et al., 2014). The depth of the potential reservoir top was used to build the thematic maps described in Section 5.

Another geological element often associated with fluid pathways is the presence of active faults. This is demonstrated by the frequent occurrence of geothermal systems within tectonically active regions and associated with geologically-young or active structures. In addition to regional geology data, mapped and interpreted geological structures and geometries at depth are important pillars for assessing geothermal resources and creating favourability maps (e.g., Noorollahi et al., 2008; Yousefi et al., 2010; Tufekci et al., 2010; Shako and Mutua, 2011). Some line of evidence also suggests that faults can also act as barriers, enhancing or preventing fluid flow according to fault zone architecture and related permeability structures (e.g., Sibson, 1990; Caine et al., 1996; Gudmundsson et al., 2001; Faulkner et al., 2010). Lithology, fault scale and geometry, self-sealing processes, fluid chemistry and degassing rates, P-T history and the stage of fault evolution may also be important controlling factors in the fault behaviour and the fluid circulation at depth. In our opinion, a general direct correspondence between a fault trace at surface and geothermal fluid flow and storage may not always be applicable, especially on a regional scale. Faults can in fact locally act as preferential recharge pathways along which cold waters infiltrate to recharge the geothermal reservoirs (e.g., Kissling and Weir, 2005). In this case, faults play a role for geothermal resource development but cannot be used as a favourable indicator.

Therefore, whether fault traces can really be considered as good drilling targets or as favourable areas for deep hydrothermal circulation is to be assessed case by case based on available evidence. Moreover, the structural complexity of Sicily can increase uncertainty around interpretation of current active kinematics, prediction of fault geometries and application of structural evidence to the development of favourability maps.

In conclusion, given the relative lack of detail and complexity of fault information in Sicily, we decided not to consider them as inputs for favourability maps of Sicily. We considered seismic hypocentral density and correlated earthquake clusters as a better signature for characterisation of deep permeability and potential fluid flow areas, as described in Subsection 4.4.

4.2. Temperature data

The data used to study the deep temperature distribution belong to one of the following three categories: i) bottom-hole temperatures (BHT) of hydrocarbon exploratory wells, ii) pool temperature measurements during production and drill-stem tests (DST) and iii) stabilized temperatures measured in geothermal wells. Since most of the boreholes had been drilled in hydrocarbon exploration sites, this new temperature analysis relied largely on BHT data. To outline the thermal regime in the sedimentary cover and in the underlying Mesozoic carbonate units, we processed the available temperatures down to 6 km depth from more than 300 wells (see Fig. 2 for well location). The corrections for the thermal disturbance caused by the drilling activity have been applied to the dataset using information on circulation time, time since circulation ceased, depth and multiple temperature records (Pasquale et al., 2012; Bullard, 1947). In cases where only single BHT records were taken, a correction approach based on an empirical correlation between the slope of the Horner plot and depth (Pasquale et al., 2008) was used. In this study, we chose to neglect corrected BHT data having errors larger than 15%. The reliability of the corrected BHTs was variable, but sufficient to highlight regional temperature anomalies. A composite plot of corrected BHTs versus depth for the deep boreholes in Sicily and surrounding seas is shown in Fig. 3.

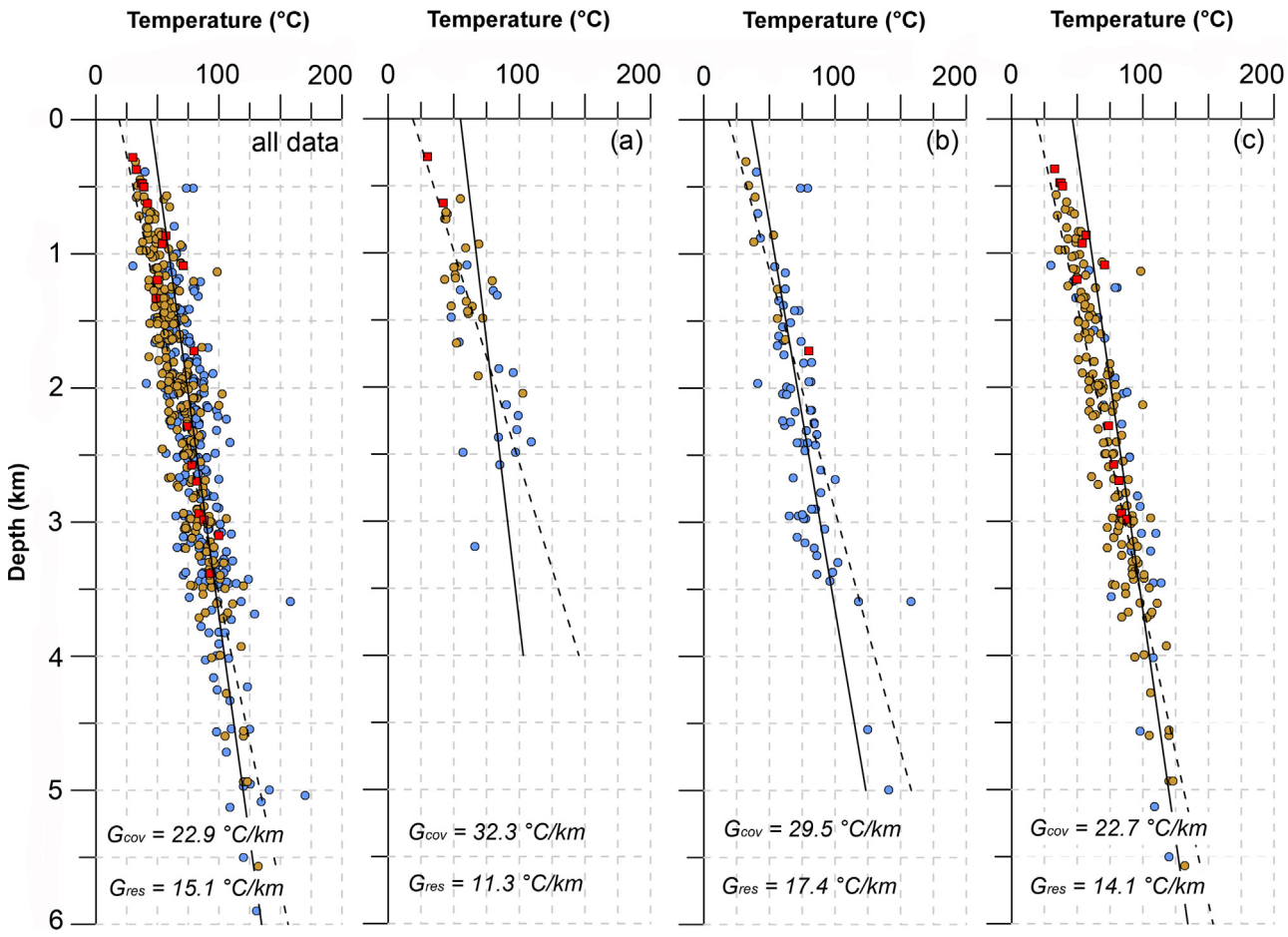

Fig. 3. Corrected Bottom-Hole Temperatures-BHT (circles) and Drill-Stem Test-DST temperatures (squares) versus depth in the whole Sicily Region (all data) and in the different sectors (a, b, c) displayed in Fig. 2. The corrected BHTs are reported by lithothermal unit in which they were acquired (sedimentary cover units: brown; carbonate reservoir units: blue). The linear regression fits of the temperature data as function of depth for both cover (dashed line) and reservoir (continuous line) units are shown together with the average thermal gradients, Gcov and Gres respectively. (For interpretation of the references to colour in this figure legend, the reader is referred to the web version of this article.)

To facilitate and simplify the thermal analysis, the geological formations were grouped in two main lithothermal units based on similarities in lithology and thermo-hydraulic properties. The boundary between the clastic sedimentary cover and carbonate reservoir units (Montanari et al., 2014) plays an important role separating the lower thermal conductivity and impervious clayey formations from the higher thermal conductivity and permeable carbonate rocks. The geothermal gradients were calculated site-by-site as a linear least-square fit to the multiple temperature–depth measurements by lithothermal units. In the sedimentary cover, we assessed the average thermal gradient assuming a mean surface temperature as a function of the elevation and latitude (Galgaro et al., 2012). In the carbonate reservoir, we constrained the thermal gradient by the temperature at its top. The temperature at the top of the carbonate reservoir was estimated by downward extrapolation of the temperatures using the thermal gradient measured in the overlying cover units. Extrapolation of geothermal gradients to depths greater than the deepest temperature measurement is an interpretation. However the deep vertical section in which we observed the temperature increase, allowed inferring an average thermal gradient representative of the whole specific lithothermal unit at the borehole location. In the wells with thermal data measured only in the carbonate reservoir, the measured thermal gradient was used to extrapolate upward the temperature at the cover-reservoir boundary. In the latter case, the thermal gradient in the sedimentary cover was inferred as the temperature difference between the ground and the top of the reservoir divided the thickness of the cover unit.

A first order of magnitude of the terrain effects due to the topographic reliefs has been evaluated by the analytical solution (Jaeger, 1965) valid for a single mountain range. The amount of the effect decreases from a sharp relief to a smooth hill. The geothermal gradient correction as function of depth and distance became lower than 10% out of a window limited in both depth and horizontal distance by the same order of magnitude of the relief height. As the geothermal gradients were computed from deep industrial temperature data in the depth range 0.8–6.0 km, the topographic correction resulted negligible. The selected boreholes are sufficiently deep that the lower section of the temperature–depth profile can be used for a suitable determination of the geothermal gradient, presumably free of the topographic effects.

We do not implicitly assume a purely conductive regime. The temperatures can be useful in the recognition of water movements (Haenel et al., 1988) as the measured geothermal gradients are the evidence of both conductive and convective heat transfer processes acting in the cover and in the reservoir units. The data revealed higher geothermal gradients in the sedimentary cover units rather than in the underlying carbonate ones. Obviously, where the thermal conductivity of rocks is unknown, the existence of fluid movements is not unequivocal, since the vertical contrast in the measured geothermal gradients can be attributed to the corresponding thermal conductivity distribution. To study

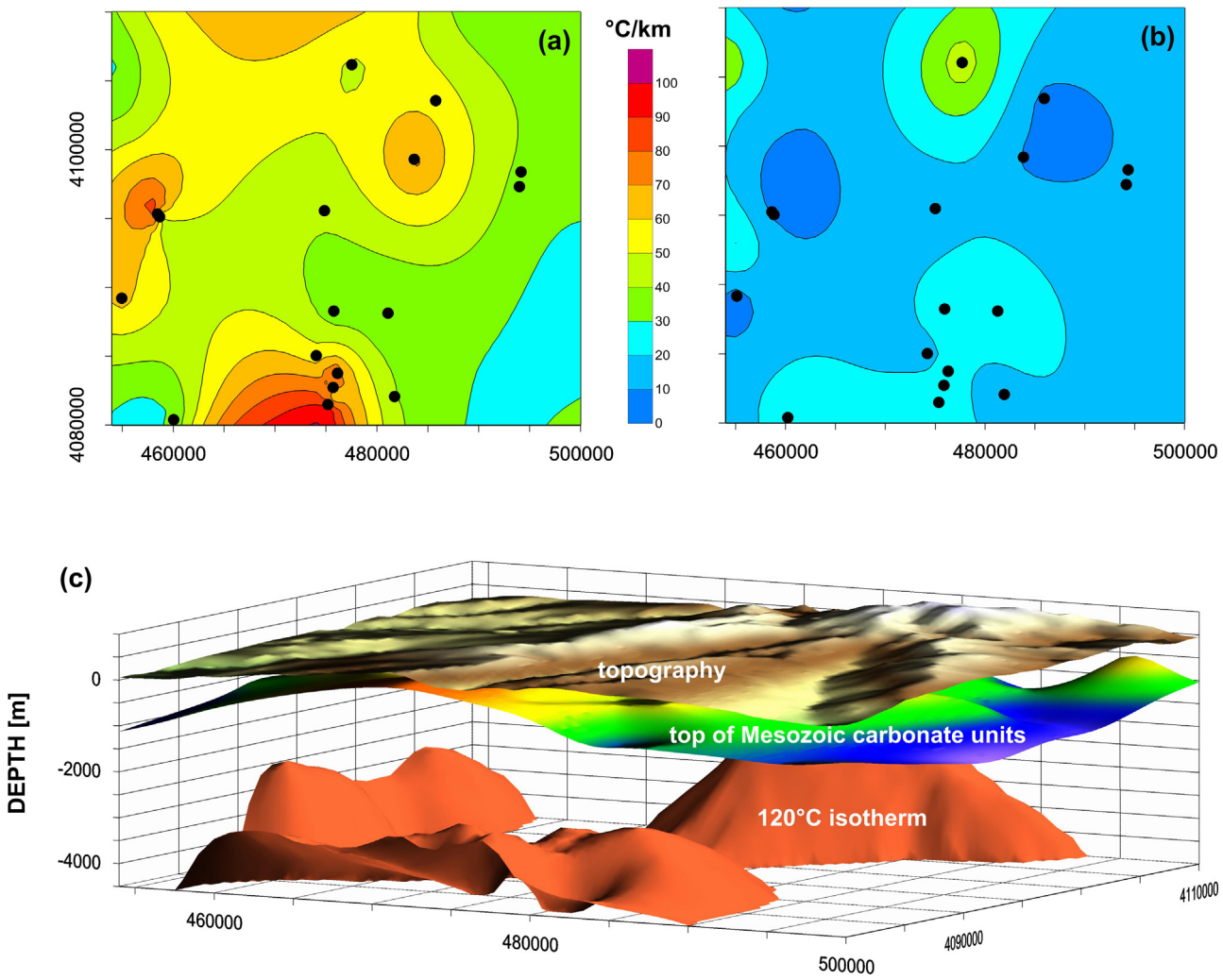

Fig. 4. Sketch map of geothermal gradient patterns (a) in sedimentary cover and (b) in the carbonate reservoir. Black dots are deep hydrocarbon wells. (c) 3D view of the top of the regional geothermal reservoir and 120 °C isotherm in a sector of Sicily.

the thermal properties of the rocks, several lithotypes were sampled in selected outcrop sites and petrophysical properties were investigated for thermal conductivity and porosity in laboratory conditions (Di Sipio et al., 2013). For the same lithotypes, the measured values corrected for porosity and saturating fluid effects are in accordance with the tabulated ones in literature (Pasquale et al., 2011; Landolt-Börnstein, 1982). Porosity-depth relationships for the main lithotypes have been obtained by the processing of the available geophysical logs (sonic and gamma ray logs). Taking into account the burial depth and temperature effects, the thermal conductivity have been evaluated for selected and representative vertical sections from lithostratigraphic information following the procedure presented in Pasquale et al. (2011). The normal distribution of the thermal conductivity values showed an average value of 2.4 ± 0.5 and 3.6 ± 0.3 W/(m K) for the sedimentary cover and the carbonate reservoir, respectively. As the vertical thermal conductivity contrast did not justify in all places such a vertical thermal gradient difference, the variation was interpreted locally as being due to convective processes occurring in the carbonate reservoir. The upwelling of geothermal fluids within the fractured carbonate rocks warms the overlying impervious cover units. The resulting thermal gradients reflect the fluid movements, they are anomalously high in the cover formations and move toward an isothermal profile in the reservoir units where the convective processes take place.

Without doubt, there are not enough measurements to characterize regionally all variations and details in temperature and geothermal gradient. We attempt to draw contours between the scattered geothermal gradient measurements applying the Kriging geostatistical method (Cressie, 1991). Geothermal gradient values are a way to quantify the depth-temperature relationship for use in evaluating geothermal resources (Pasquale et al., 2013; McPherson and Chapman, 1996; Deming and Chapman, 1988). To create the first subsurface temperature model for the entire Sicily a combined geothermal gradients interpolation and downward temperature extrapolation supported by geologic knowledge approach was chosen. Thus actual temperature field derives by a combination of the annual mean surface temperatures and regionally varying geothermal gradients measured in the deep boreholes in relationship with the cover-reservoir discontinuity depth map from Montanari et al. (2014). Although a contour map is an interpretation, we used the interpretative geothermal gradient maps of the sedimentary cover and reservoir units to compute the temperature distribution down to a depth of 5 km on a mesh grid of $1000 \times 1000 \times 100\ m^3$ along the latitude, longitude and depth, respectively.

The gradient maps, shown in Fig. 4, and the temperature model were used to obtain three thematic maps combined with other information in the favourability computation, as described in Section 5.

4.3. Geochemical data

In order to assess the geothermal favourability of Sicily using geochemical parameters of natural thermal manifestations, published geochemical and isotopic data were collected and organized. The basis of this collection was the nationwide geothermal database managed and updated by the Italian National Research Council and researchers over the years (ENEL et al., 1988; Barbier et al., 2000; Manzella, 2013).

With the exception of the Caltanissetta basin in central Sicily, where thick clay-rich formations do not allow deep confined fluids to escape to the surface because of low-permeability, and where CH_4-rich fluids hosted in the sediments are expelled even violently (such as occurred at S. Barbara village near Caltanissetta, in 2008, described in Madonia et al., 2011), there are several well-known thermal springs in both eastern and western Sicily (see Fig. 2). Many of these springs emerge at the edges and at the foot of the outcrops of the Mesozoic carbonate units, prevalently at topographically low areas (e.g., Segesta) or near coastal areas (e.g., Termini Imerese, Alì Terme and Sciacca). Others thermal springs surround Mt. Etna volcano and the Quaternary Hyblean volcanics in south-eastern Sicily, where there are fumaroles and CO_2-rich dry-gas vents, respectively (Chiodini et al., 1996; D'Alessandro et al., 1996; D'Alessandro et al., 1997; Allard et al., 1997; Caracausi et al., 2003a,b; Grassa, 2001; Pecoraino and Giammanco, 2005; Tassi et al., 2012).

The chemical data of thermal springs and gas emergences were organized into a GIS database of more than 400 analyses, sometimes heterogeneous in terms of analysed components. The dataset of each site includes flow rate, temperature, *p*H, electrical conductivity, main and trace chemical components and isotopic compositions. Because of redundancy, the dataset was screened to select the best analyses. For water samples we only used analyses with an ionic unbalance of less than 5%, whereas for gases, we selected samples where it was evident that no air contamination had occurred during the sampling.

Within the framework of this study we decided to focus only on two parameters: (i) the calculated partial pressure of CO_2 in the thermal springs (and/or shallow wells) and (ii) the $^3He/^4He$ isotopic ratio of gas discharges (as R/Ra where the ratio R in the sample is normalized to the atmospheric Ra ratio = 1.39×10^{-6}). In fact, the $^3He/^4He$ ratio is a good indicator of the presence of mantle magmas residing in the crust (e.g., O'Nions and Oxburgh, 1988) and, together with CO_2, it can be a good indicator of degassing hydrothermal/metamorphic systems, possibly located around and above the magma chamber itself (e.g., Marty and Jambon, 1987).

The R/Ra ratio of the dry gas vents and/or dissolved gas in thermal waters varies from 0.08 in the methane-rich emissions related to the post-orogenic Mio-Pliocene sedimentary sequences (Parello et al., 2001), to values greater than 7.0 in the fumaroles of Mt. Etna (Hooker et al., 1985; Sano et al., 1989; Marty et al., 1994; Tedesco, 1997). The highest value of 7.3 has been measured at Pantelleria, a volcanic island in the Sicily channel (Parello et al., 2000). Considering the R/Ra ratio of the upper mantle gas close to 8.0 in MORB and the crustal ratios less than 0.2, the high ratio and therefore the strong ^3He-signature of gases discharged in many places in Sicily indicates an origin from the mantle. In order to draw the distribution map of the ratio, the data were interpolated using the Kriging method. Given the scattered distribution of the data in the territory, insufficient to delineate possible anisotropic trends, we adopted an omnidirectional spherical model. This interpolation method enabled us to obtain a raster map with 1000 m x 1000 m sized cells, from 24 input points. The interpolated R/Ra values in areas with poor data coverage are, of course, more uncertain than areas with good data coverage and, therefore, should be interpreted with caution. Further details on how we used He ratios for favourability maps are provided in Section 5 and Table 1.

Table 1
Scores of classes and weights W1 and W2 for Thematic map and Layers of evidence respectively, used in the favourability analysis.

Layer of evidence	W1	Thematic map	W2	Score				
				5 (Very high)	4 (High)	3 (Medium)	2 (Low)	1 (Very low)
Effective reservoir	0.4	Depth of effective reservoir's top (m)	–	≤1500	1500–2500	2500–3500	3500–4500	>4500
Thermal signature	0.3	Temperature at reservoir's top (°C)	0.5	≥190	160–190	140–160	120–140	<120
		Depth of reservoir's top (m)	0.5	500–1500	1500–2500	2500–3500	3500–4500	>4500 and ≤500
Permeability indication	0.15	Hypocentres density (number/km2)	0.5	>10	3–10	1–3	0.1–1	≤0.1
		Rg	0.5	≥3.5	2.5–3.5	1.8–2.5	Cover absent	<1.8
Geochemical favourability	0.15	He R/Ra	0.5	≥5.0	4.0–5.0	3.0–4.0	1.5–3.0	<1.5
		log(pCO2) (atm)	0.5	>0.0	0.0—1.0	−1.0—2.5	−2.5—3.5	<−3.5

Four main areas with relevant ^{3}He-enrichments were identified in mainland Sicily: (i) the Sciacca area (SW Sicily) where the R/Ra value is >2.6 (Caracausi et al., 2005; Capaccioni et al., 2011); (ii) the active volcanic area of Mt. Etna with an R/Ra value of about 7 (Allard et al., 1997); (iii) the Naftia-Palagonia area in the Hyblean Mts (Polyak et al., 1981), located 40 km south of Mt.Etna volcano with similar R/Ra values to the ones of Mt. Etna; (iv) the Peloritani Mts (NE Sicily) with values of R/Ra = 2.5 at Capo Calavà (Sano et al., 1989) and R/Ra = 2.14 at Rodì Milici (Giammanco et al., 2008).

Regarding the calculated CO_2 partial pressure in thermal springs, we processed the spring data using the Phreeqc-2 Speciation Program (Parkhurst and Appelo, 1999). Data were plotted as $\log(pCO_2)$ and interpolated using the same Kriging method described for the ^{3}He/^{4}He ratio. The maximum values, linked also to the presence of several CO_2 gas vents, are located: (i) in eastern Sicily along the Aeolian-Tindari-Letojanni fault system (Giammanco et al., 2008), (ii) around the Etna Volcano and the Hyblean Quaternary volcanics (De Gregorio et al., 2002) and (iii) at Sciacca (Capaccioni et al., 2011). Conversely, the minimum values are centred in the Caltanissetta basin, the Hybean Plateau and the thermal springs in the N–NW sector of Sicily.

We found that some areas (in addition to the active volcanic island of Vulcano and Pantelleria), i.e.: Sciacca, Naftia-Palagonia, Mt. Etna area, Mt. Peloritani area have the maximum anomalous values of both the selected parameters. This suggests that both elements have a common pathway, typically where the hydrothermal alteration of relatively shallow limestone producing CO_2 is triggered by underneath mantle magmas intruded and residing in the crust (Barnes et al., 1978). Similar occurrences have already been reported in many other volcanic and geothermal areas of central-southern Italy (Minissale, 2004; Giammanco et al., 1998 and references therein). The existence of deep hydrothermal system is supported, in these areas, not only by the presence of high ^{3}He/^{4}He ratio and high pCO_2 values, but also by the δ^{13}C value of CO_2 values which clearly indicate a hydrothermal relatively deep contribution for the CO_2 in many site of the island (Grassa et al., 2006; Giammanco et al., 1998).

4.4. Seismological data

Permeability constitutes a critical reservoir parameter as it plays a fundamental role in heat and mass transfer and it can ultimately determine the economic viability of a geothermal prospect. Estimating rock permeability is difficult, as naturally-fractured carbonates (the main reservoir in Sicily) exhibit substantial and unpredictable spatial variations. Due to the scale of investigation, a first-order assessment of this property has to be evaluated from regional information, identifying permeable zones acting as preferential pathways for hydrothermal circulation. Given the close relationship between active fault-fracture systems, permeability and fluid circulation, pointed out by several authors (e.g., Sibson, 1996; Curewitz and Karson, 1997; Norton and Knapp, 1997), and the potential uncertainty in the interpretation of geological-structural models of Sicily, we focused our structural interpretation on seismological data as a possible indicator of open fracture systems and high permeability. The advantage of seismicity is the well proven connection with active faults and fracture networks (e.g., Sibson, 1996) Sicily is characterized by active and complex tectonics, and it is one of the most seismically active areas of the Mediterranean with large historical tectonic earthquakes (Boschi et al., 1997) as well as seismic swarms.

For example, Mt. Etna undergoes frequent seismic swarms linked to the opening of eruptive fracture systems (e.g., see Patanè et al., 2003, referring to the 2001 eruption). Giammanco et al. (2008) pointed out the local interaction between high pressure fluids and normal faults in triggering the highly-clustered swarm earthquakes located at a shallow depth (7–12 km) in an area of the western Peloritani Mts (north-eastern Sicily).

Considering secondary fracture-related permeability as a predominant factor within the regional geothermal reservoir and the above-mentioned relationship between seismic activity and fluid circulation, we used the earthquake epicentre density as an indicator of possible fluid flows. The epicentre data were extracted from the "CSI 1.1, Italian Seismicity Catalogue" (Castello et al., 2006) and the "ISIDe Database, Italian Seismic Instrumental and parametric Data-basE" (ISIDe Working Group INGV, 2010), both developed and managed by the Italian National Institute of Geophysics and Volcanology (INGV), which provide the parameters of all earthquakes registered in Italy from 1981 to 2002, and from 2005 to January 2013, respectively.

To compute the epicentre density, the database was filtered by considering only the seismic events that have occurred in mainland Sicily up to a depth of 10 km below ground level (b.g.l.). The resulting dataset consists of 5723 records with a magnitude ranging from 0.5 to 4.7, and was used to compute the epicentre density map.

5. Layers of evidence

Having decided to use the Index Overlay (IO) method (Bonham-Carter et al., 1994) to produce the favourability map for conventional geothermal systems, we combined different maps using a system of weighting and scoring. On the basis of the data sources described in Section 4, seven thematic maps were created, classified, scored and weighted. The classifications for each map consisted of identifying five ranges of values (classes). The classes were scored from 1-to-5, "Very low" (least favourable area) to "Very high" (most promising area) respectively. In order to combine the maps, each was weighted with a value ranging from 0 to 1 (Table 1).

The workflow for the favourability map was organized into two stages, as shown in Fig. 5. In the first stage, seven thematic maps were used to produce four layers of evidence. These layers of evidence are related to favourable factors and refer to: (i) the effective reservoir, (ii) the thermal signature, (iii) the permeability indication and (iv) the geochemical favourability.

The "effective reservoir" layer was derived from the GIS layer intersection between the depth of the reservoir top and the 120 °C isotherm depth. The other three layers of evidence were gathered using three different IO computations.

The four layers of evidence were combined in the second stage by further IO computation, to produce the final map.

Before discussing the final favourability map, in the following subsections we will describe the meaning of each layer of evidence and how it was obtained.

5.1. Effective reservoir

Considering the regional carbonate reservoir and the temperature distribution pattern described in Subsection 4.2, we neglected the volume of the potential reservoir that are colder than 120 °C. This minimum temperature was chosen on the basis of knowledge driven technical and economic factors.

We performed a layer intersection analysis of two thematic maps (Top reservoir depth and 120 °C isobath) to compute the effective reservoir layer of evidence (Fig. 6).

A depth-based scoring of this layer was performed by considering the drilling costs as a function of well length. The depth to be drilled to encounter the effective reservoir was classified (see Table 1) by considering an exponential function describing the average-completed well costs as a function of depth (IFC, 2013; Augustine et al., 2006; Huenges, 2010). Regarding the maximum

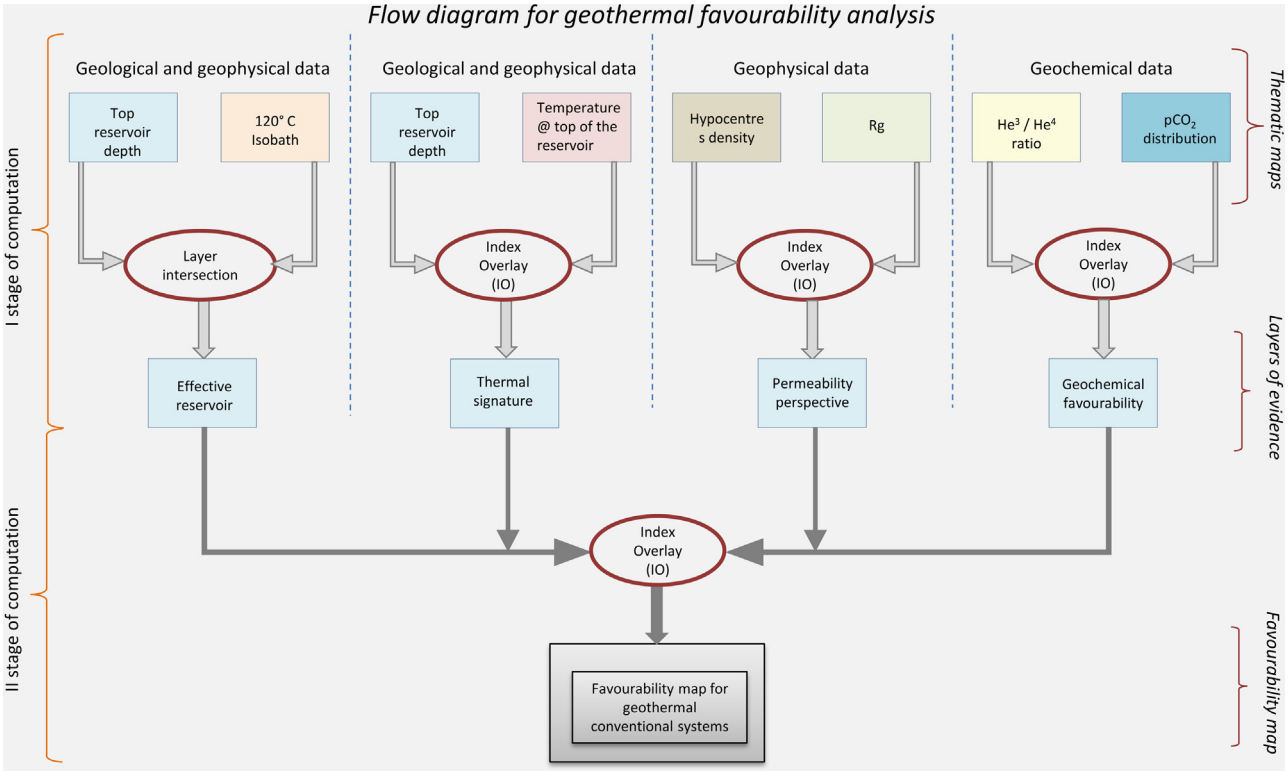

Fig. 5. Flow diagram for geothermal favourability analysis.

drilling depth, a depth higher than 4000–4500 m is considered critical in terms of cost for commercial purposes, and worldwide most geothermal wells exploit resources shallower than 3500 m. However, deep geothermal wells have been drilled at depths ranging from 4300 to 5400 m, in the geothermal fields of Larderello (Italy), Habanero (Cooper Basin, Australia), Fenton Hill (USA), Basel (Switzerland), and Soultz (France). The resulting reclassified map is shown in Fig. 7.

5.2. Thermal signature

The thermal structure of the reservoir is an important factor for classifying the geothermal favourability. We used an IO model to build the thermal signature by combining the temperature at the top of the potential reservoir and the depth of this top. The classification and scoring used for the reservoir's depth is the same as used for the effective reservoir (Table 1), but we also took into account the unfavourable effect of seeping meteoric water recharge where carbonates crop out or have a thin sedimentary cover (<500 m).

To classify the temperature at the top of the reservoir, we considered temperatures lower than 120 °C as the least favourable class, as explained in Subsection 5.1. The 140 °C and 160 °C temperature limits chosen are somewhat arbitrary and may be moved either way by about 10 °C. The upper limit of 190 °C depends on technical and financial aspects regarding mainly the possibility of exploiting "Flash" technology and self-flowing wells (Sanyal, 2005). Fig. 8 shows the thermal signature map.

5.3. Permeability indication

The permeability indication layer of evidence is the result of an IO computation between two thematic maps: (i) the earthquakes density analysis and (ii) the geothermal gradient ratio analysis.

A density analysis of earthquake epicentres was performed in GIS to create a density thematic map using a "Kernel Density Estimation" tool. Following the conservative criterion shown by Noorollahi et al. (2007), with regard to the distance between geothermal wells and active faults, we calculated the density map by setting a search radius (Kernel bandwidth) of 2000 m centred on each single epicentre. A "Uniform Kernel Shape" function was chosen, which controls the rate at which the influence of a point decreases with the distance. The result is a raster map

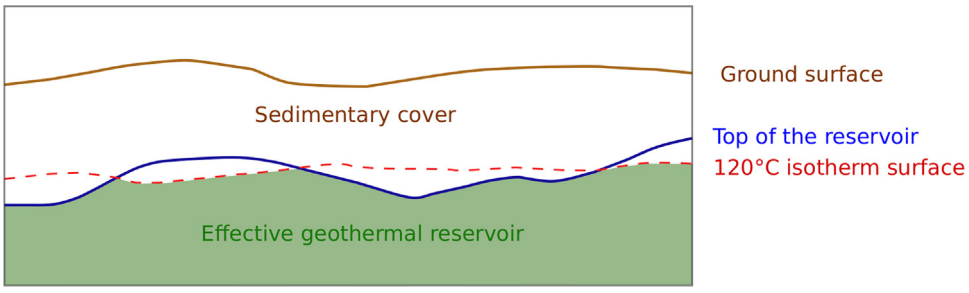

Fig. 6. Cross-section explaining the concept of *effective reservoir*.

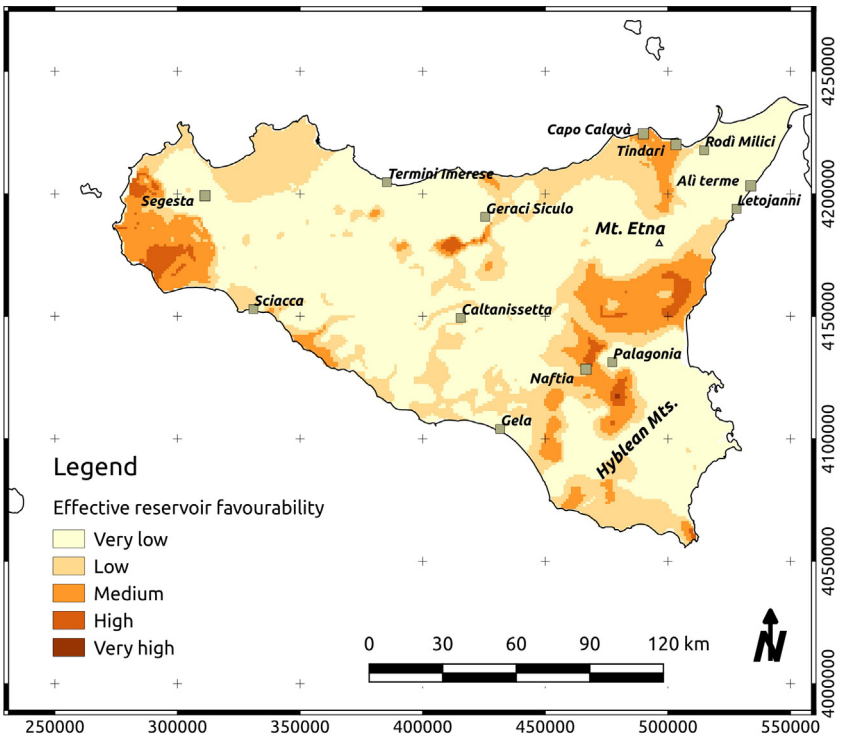

Fig. 7. Reclassified map of the *effective reservoir* layer of evidence.

characterized by a continuous distribution of density values. Considering that higher density values could be related to higher permeability, the density map was reclassified (Table 1), from the first least favourable class, corresponding to areas without seismic events up to 0.1 values, to the fifth most favourable class with values up to 17.4.

The observed low thermal gradient in the deep carbonate reservoir and high values in the overlying impermeable formations could be used as a permeability indicator (Pasquale et al., 2013; Saar, 2011). In a steady-state conductive layered model without an internal heat source, since the heat flowing through the boundaries is constant, for a given heat-flow density the geothermal gradients

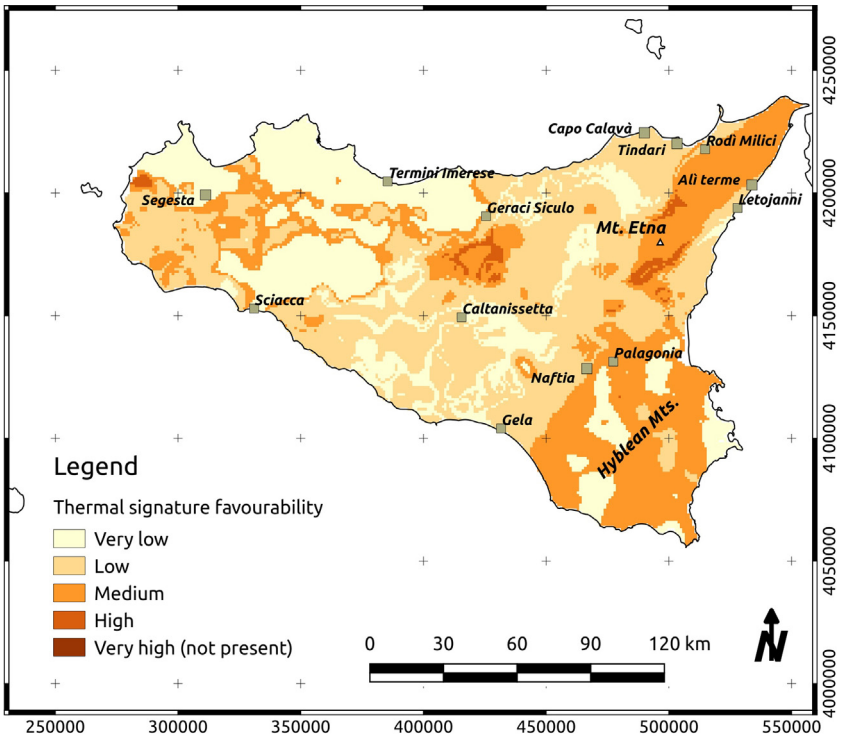

Fig. 8. Reclassified map of the *thermal signature* layer of evidence.

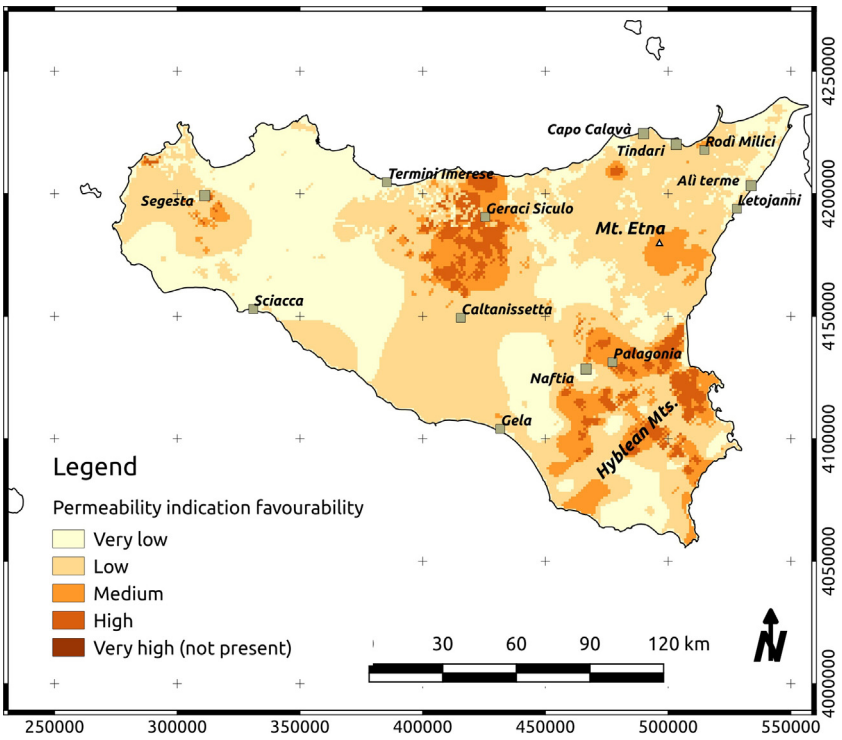

Fig. 9. Reclassified map of the *permeability indication* layer of evidence.

are inversely proportional to the thermal conductivities. For a two-layer model, we have:

$$\mathrm{Rg} = \frac{k_2}{k_1} = \frac{G_1}{G_2} \tag{2}$$

where, k is the thermal conductivity, G the geothermal gradient, and subscripts 1 and 2 correspond to the sedimentary cover and reservoir units, respectively. In selected wells, the thermal conductivity profiles are evaluated by inverting the geophysical logs and stratigraphic information. The normal distribution of the thermal conductivity displays an average value of 2.4 ± 0.5 W/(m K) and 3.6 ± 0.3 W/(m K) for the sedimentary cover and the carbonate reservoir, respectively. A computed value of 1.5 ± 0.3, given by the ratio between the average reservoir and sedimentary cover thermal conductivities, is taken as a reference value to distinguish pure conductive from mixed conductive/convective thermal regimes. Almost all temperature–depth profiles are convex upward, i.e. the temperature gradient is higher in the cover than in the reservoir. The geothermal gradient maps are used to compute the parameter Rg. The Rg values, ranging from 1.2 to 1.8, can be explained by the thermal conductivity differences between the clay-rich terrigenous rocks and the overlying Mesozoic carbonates. Higher ratios can be interpreted as due to ascending/descending water movements occurring in the permeable reservoir. Ratios lower than 1.2 relate to ineffective cap-rock and descending water in a sedimentary cover region. Fig. 9 shows the permeability indication map for Sicily.

5.4. Geochemical favourability

The geochemical thematic maps of the $^3He/^4He$ ratios (as R/Ra) and the pCO_2 described in 4.3 were quantitatively classified and combined using the IO method to compute the geochemical favourability layer of evidence (Table 1) (Fig. 10). The reasons for the reported limits for the R/Ra are as follows. The ratio of long circulating fluids in the crust tends to zero, as the ^4He is continuously formed by radioactive decays, whereas the ^3He flux from the mantle reflects the primordial helium.

Ratios less than 0.05 are typically crustal, whereas ratios of more than 0.2 suggest an increase in primordial ^3He from the mantle (O'Nions and Oxburgh, 1988). As the R/Ra ratios in typical Neapolitan volcanic areas (Ischia, Phlegrean Fields and Vesuvius) are a little more than 2.0 because of the presence of high crustal contamination (Tedesco et al., 1990), we chose this value as a possibly good minimum ratio to limit the best class in Sicily as well. The two classes bounded between the ratios of 0.2 to 2.0, are somewhat arbitrary and may not reflect really large differences in geochemical terms.

Regarding the calculated pCO_2, in many thermal waters of central Italy, it is quite common to have positive (>0) logarithmic values (meaning $pCO_2 > 1$ atm and therefore free CO_2 bubbling in the atmosphere), and this can be considered the best indication of waters saturated with free CO_2, especially near volcanic areas. The lower limit (<−3.5) represents a cold, shallow water equilibrated with atmospheric CO_2. Deep circulating water where the only dissolved gas phase is air (dissolved in rainfalls), and the only CO_2 entering into the hydrological system is produced by bacteria in the soil are characterized by pCO_2 values of solutions near -3.5. As for helium, the intermediate limits can be considered as somewhat arbitrary, if we consider that the degassing of fluids from the earth, especially in volcanic areas, is often connected to single faults and/or fault systems.

6. Results: the favourability map

Following the data integration described in Section 5, we obtained the geothermal favourability map shown in Fig. 11.

The map shows the areas of Sicily where geological conditions are likely to host hydrothermal systems at depth, and are thus suitable for a more detailed exploration. The map also shows a correlation with the heat flow distribution in Fig. 2.

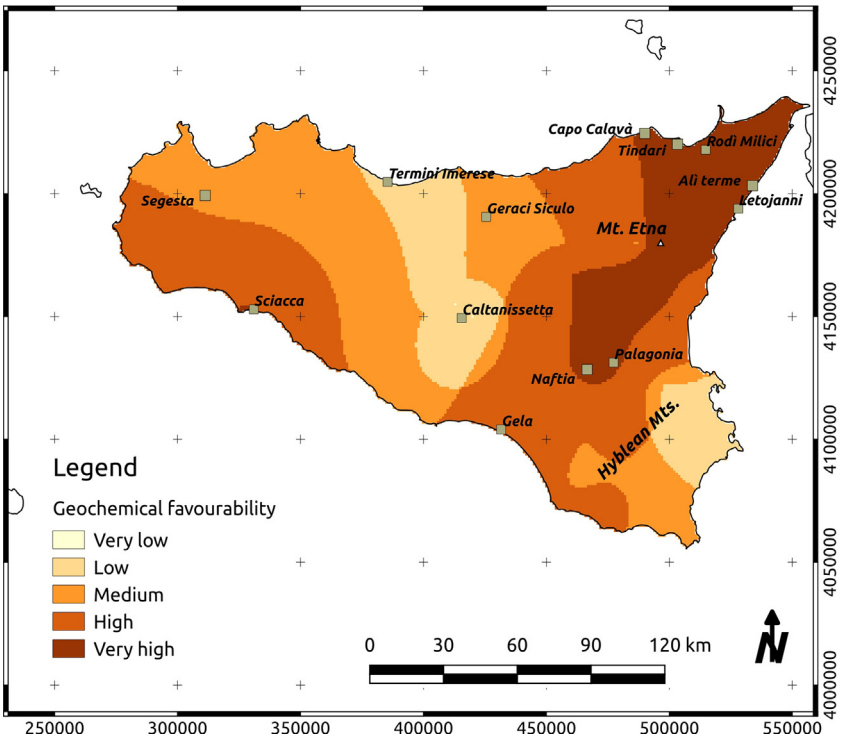

Fig. 10. Reclassified map of *geochemical favourability* layer of evidence (Very low class is present in only 2 pixel near Caltanissetta).

Low favourability values are located mainly where the regional reservoir geological units crop out (i.e. the likely recharge areas), and in the Caltanissetta basin where the reservoir is very deep and there is a low geothermal gradient in the sedimentary cover.

The map highlights medium and highly favourable areas in eastern Sicily, from Mt. Etna towards the town of Gela, and in the westernmost area of Sicily. Some other promising areas occur in the centre of Sicily near the village of Geraci Siculo and on the south-west coast, close to thermal springs in Sciacca.

7. Discussion on the accuracy of favourability map

The reliability of the favourability map relates mainly to the accuracy of data and the number of measuring sites. Favourability

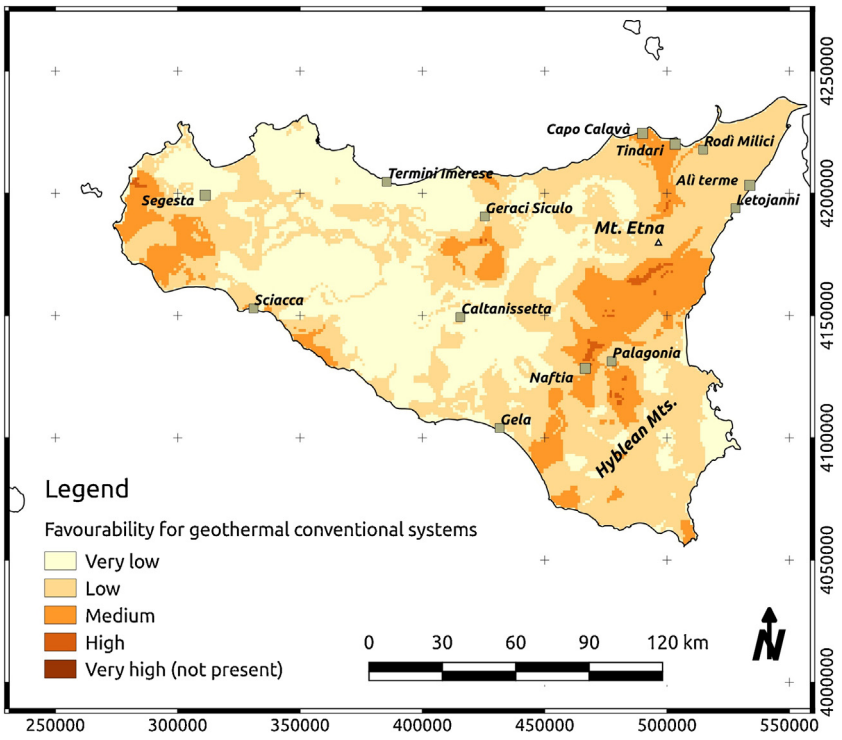

Fig. 11. Favourability map for geothermal "conventional" hydrothermal systems in Sicily.

Table 2
Reliability assigned to each source of data for the computation of the accuracy map.

Class of data	Source of data	Spatial operation	Reliability (from 0 to 1)	Weight
Geological data	Reservoir outcrops	Areas of reservoir outcrop	1	0.3
		3 km buffer ray	0.75	
Geological data	Deep wells	3 km buffer ray	1	
Geological data	Shallow wells	3 km buffer ray	0.5	
Geological data	Seismic and geologic cross-sections	3 km buffer ray	0.65	
Geological data	Interpreted gravimetric data	Area coverd by grav data	0.4	
Seismological data	Hypocentres	2 km buffer ray	1	0.15
Geochemical data	Geochemical sampling point	2,5 km buffer ray	1	0.15
Thermal data	Wells logs	Interpolation: Inverse distance method	average of 3 factors	0.4

computed in sectors well constrained by the simultaneous existence of geological, thermal, seismological and geochemical data has a greater degree of reliability than sectors where thematic maps are obtained through extrapolation techniques, as no experimental data are available. We thus applied simple spatial operators (e.g., buffer, merge, union) to obtain the accuracy of: (i) geological data, (ii) geochemical data, (iii) seismological data, and (iv) thermal data.

The final accuracy map was computed with an IO technique, by combining the accuracy of the four classes of data listed above, which was then overlaid onto the favourability map to highlight the best constrained areas.

All the data were buffered and then scored, from 0 to 1, following knowledge-driven criterion as with the computation of the favourability map. The final IO analysis was carried out taking into account, for each class, the weight shown in Table 2.

For the geological reliability layer, after buffering and scoring each source data the following were merged: (i) reservoir outcrops, (ii) deep wells, (iii) shallow wells, (iv) seismic and geological cross sections and (v) gravimetric data.

For geochemical sampling points and hypocentres, a simple buffer for each one was computed, and the maximum score of 1 was assigned to the buffer areas produced.

For thermal data, the evaluation criteria were based on three basic parameters: (i) number of BHT measurements, (ii) length of interval along which the thermal gradient is derived and (iii) maximum BHT depth. Finally, the scores of the above three parameters were averaged to obtain the final score for each well site. We set a score of 1 for a minimum number of 3 BHTs, 0.75 for 2 BHTs, and 0.5 when only one BHT is available. Since the representativeness of the computed thermal gradient in the selected geological layer increases with the length of the interval along which it is derived, we set a score of 1 when the interval length is equal or greater than 1 km, otherwise we infer a score equal to the interval length in km. Because of the uncertainty with downward temperature extrapolation increases with the distance from the last measuring point, we set a score given by the ratio between the depth of the deepest BHT reading and a fixed depth of 4500 m. When the depth of the deepest BHT is greater than 4500 m, we fix a score of 1. An interpolation, using an Inverse Distance method, on the assigned variable score allowed us to obtain the spatial distribution of the reliability for thermal data.

The accuracy of the favourability map shows only areas with an accuracy higher than 0.5 (Fig. 12).

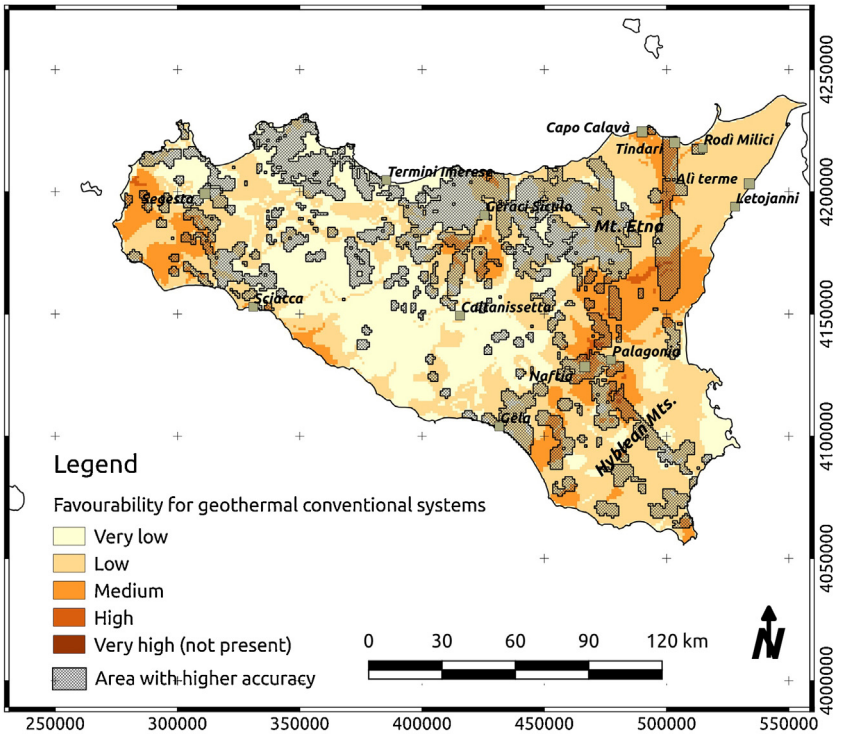

Fig. 12. Accuracy of favourability map. Areas well constrained by direct or indirect data are shown in grey.

8. Conclusions

The last official geothermal assessments have performed a qualitative ranking of Italian territories up to a 3 km depth (ENEL et al., 1988; Cataldi et al., 1995). They were based on hydrological characteristics and temperatures within the regional aquifer.

In this paper we have proposed an approach for a fully integrated analysis in order to classify the hydrothermal resources hosted by regional reservoirs and suitable for power production and applied it to Sicily. In addition to using geological and thermal data, we introduced: (i) the unconventional new parameter "effective reservoir" (based on temperature constrain), (ii) the permeability indication and (iii) geochemical favourability.

The approach here described integrates direct and indirect information and exploits modern geostatistical and GIS techniques. The result is the geothermal favourability map of Sicily where locations are ranked in five classes from "very low" to "very high".

The novelty, here, is: (i) the adaptation of a methodology to the specific conditions of the study area, (ii) the definition of innovative parameters for geothermal assessments, (iii) the choice of inputs and (iv) our weighting and ranking criteria.

Our tool is highly flexible: with a simple reclassification it can show future scenarios taking into account new technologies and possibly lower costs.

Our data integration tool is not based on a broadly distributed dataset. Information was extrapolated in areas where information is lacking, and the results did not have the same consistency throughout the region. The solution to this problem would be to drill evenly-distributed new exploration wells and to acquire evenly-distributed indirect information. This would be prohibitive due to the high costs of drilling and exploration compared to the return on the investment revenues. By combining the accuracy and favourability we showed the most constrained areas (Fig. 12).

The favourability map for geothermal conventional system, obtained for the Sicily mainland (Fig. 11), highlights areas where investment in knowledge has the highest probability of being productive.

Acknowledgement

This work was carried out within the framework of the GEOTHERMAL ATLAS OF SOUTHERN ITALY Project, one of six Projects constituting the Program "CNR per il Mezzogiorno" of the Italian National Research Council, aimed at improving know how in the fields of advanced technology for energy efficiency, environmental protection, agro-food innovative methodologies for the Made in Italy and biotech medicine production.

References

Accaino, F., Catalano, R., Di Marzo, L., Giustiniani, M., Tinivella, U., Nicolich, R., Sulli, A., Valenti, V., Manetti, P., 2011. A crustal seismic profile across Sicily. Tectonophysics 508, 52–61.

Agterberg, F.P., 1989. Computer programs for mineral exploration. Science 245, 76–81.

Allard, P., Jean-Baptiste, P., D'Alessandro, W., Parello, F., Parisi, B., Flehoc, C., 1997. Mantle-derived helium and carbon in groundwaters and gases of Mount Etna, Italy. Earth Planet. Sci. Lett. 148, 501–516.

Augustine, C., Tester, J.W., Anderson, B., Petty, S., Livesay, B., 2006. A comparison of geothermal with Oil and Gas well drilling costs. In: 7th Proceedings, Thirty-First Workshop on Geothermal Reservoir Engineering, Stanford University, Stanford, California, January 30-February 1 2006, SGP-TR-179.

Barbier, E., Bellani, S., Musmeci, F., 2000. The Italian geothermal database. In: Proceedings of World Geothermal Congress 2000, Japan, June 2000, pp. 3991–3995.

Barnes, I., Irwin, W., White, D., 1978. Global distribution of CO_2 and major zones of seismicity. U.S. Geol. Surv., Open-File Rep., 39–78.

Bello, M., Franchino, A., Merlini, S., 2000. Structural model of eastern Sicily. Mem. Soc. Geol. Ital. 55, 61–70.

Bertani, R., 2012. Geothermal power generation in the world 2005–2010 update report. Geothermics 41, 1–29.

Bonham-Carter, G.F., Agterberg, F.P., Wright, D.F., 1988. Integration of geological datasets for gold exploration in Nova Scotia. Photogramm. Eng. Remote Sens. 54, 1585–1592.

Bonham-Carter, G.F., 1991. Integration of geoscientific data using GIS. In: Maguire, D.J., Goodchild, M.F., Rhind, D.W. (Eds.), Geographical Information Systems: Principles and Applications. Longman, Essex, pp. 171–184.

Bonham-Carter, G.F., 1994. Geographical Information Systems for Geoscientists: modelling with GIS. Computer Methods in the Geosciences, 13. Pergamon, New York, pp. 398.

Bonham-Carter, G.F., Reddy, R.K.T., Galley, A.G., 1994. Knowledge-driven modeling of volcanogenic massive sulphide potential with a geographic information system. In: Kirkham, R.V., Sinclair, W.D., Thorpe, R.I., Duke, J.M. (Eds.), Mineral Deposit Modeling, 40. Geological Association of Canada, pp. 735–749 (Special Paper).

Boschi, E., Guidoboni, E., Ferrari, G., Valensise, G., Gasperini, P., 1997. Catalogo dei forti terremoti in Italia dal 461 a.C. al 1990. ING and SGA, pp. 644.

Bullard, E.C., 1947. The time necessary for a borehole to attain temperature equilibrium. Mon. Not. R. Astron. Soc. 5, 127–130.

Caine, J.S., Evans, J.P., Forster, C.B., 1996. Fault zone architecture and permeability structure. Geology 24, 1025–1028.

Capaccioni, B., Vaselli, O., Tassi, F., Santo, A.P., Huertas, A.D., 2011. Hydrogeochemistry of the thermal waters from the Sciacca geothermal field (Sicily, southern Italy). J. Hydrol. 396, 292–301.

Caracausi, A., Favara, R., Giammanco, S., Italiano, F., Nuccio, P.M., Paonita, A., Pecoraino, G., Rizzo, A., 2003a. Mount Etna: Geochemical signals of magma ascent and unusually extensive plumbing system. Geophys. Res. Lett. 30 (2), 1057.

Caracausi, A., Italiano, F., Paonita, A., Rizzo, A., Nuccio, P.M., 2003b. Evidence of deep magma degassing and ascent by geochemistry of peripheral gas emissions at Mount Etna (Italy): assessment of the magmatic reservoir pressure. J. Geophys. Res. 108 (B10), 2463, http://dx.doi.org/10.1029/2002JB002095.

Caracausi, A., Favara, R., Italiano, F., Nuccio, P.M., Paonita, A., Rizzo, A., 2005. Active geodynamics of the central Mediterranean Sea: tensional tectonic evidences in western Sicily from mantle-derived helium. Geophys. Res. Lett. 32, L04312.

Carapezza, M., Cusimano, G., Liguori, V., Alaimo, R., Dongarrà, G., Hauser, S., 1977. Nota introduttiva allo studio delle sorgenti termali dell'isola di Sicilia. Boll. Soc. Geol. It. 96, 813–836.

Castello, B., Selvaggi, G., Chiarabba, C., Amato, A., 2006. CSI Catalogo della sismicità italiana 1981–2002, versione 1.1. INGV-CNT, Roma. ⟨http://csi.rm.ingv.it/⟩ (accessed October 2013).

Catalano, R., 2004. Geology of Sicily: an introduction. Bocconea 17, 33–46.

Catalano, R., 2013. Sicily's fold/thrust belt. An introduction to the field trip. In: Catalano, R., Agate, M., Albanese, C., Avellone, G., Basilone, l., Morticelli, G.M., Gugliotta, C., Sulli, A., Valenti, V., Gibilaro, C., Pierini, S. Walking along a crustal profile across the Sicily fold and thrust belt. AAPG International Conference & Exhibition - Milan 2011 Geological field trips Vol.318 5 No.2.3, pp 16 of 32.

Catalano, R., D'Argenio, B., 1982. Schema geologico della Sicilia. In: Catalano, R., D'Argenio, B. (Eds.), Guida alla Geologia della Sicilia Occidentale. Società Geologica Italiana, Palermo.

Catalano, R., Merlini, S., Sulli, A., 2002. The structure of western Sicily, central Mediterranean. Pet. Geosci. 8, 7–18.

Catalano, R., Agate, M., Albanese, C., Avellone, G., Basilone, l., Morticelli, G.M., Gugliotta, C., Sulli, A., Valenti, V., Gibilaro, C., Pierini, S., 2013. Walking along a crustal profile across the Sicily fold and thrust belt. AAPG International Conference & Exhibition - Milan 2011 Geological field trips Vol.318 5 No.2.3, 213 pp.

Cataldi, R., Mongelli, F., Squarci, P., Taffi, L., Zito, G., Calore, C., 1995. Geothermal ranking of Italian territory. Geothermics 24 (1), 115–129.

Chung, C.F., Jeerson, C.W., Singer, D.A., 1992. A quantitative link among mineral deposit modelling, geoscience mapping, and exploration-resource assessment. Econ. Geol. 87, 194–197.

Chiodini, G., D'Alessandro, W., Parello, F., 1996. Geochemistry of gases and waters discharged by the mud volcanoes at Paternò, Mt. Etna (Italy). Bull. Volcanol. 58, 51–58.

Coolbaugh, M.F., Taranik, J.V., Raines, G.L., Shevenell, L.A., Sawatzky, D.L., Minor, T.B., Bedell, R., 2002. A geothermal GIS for Nevada: defining regional controls and favorable exploration terrains for extensional geothermal systems. Geotherm. Res. Council Trans. 26, 485–490.

Coolbaugh, M.F., Shevenell, L.A., 2004. A method for estimating undiscovered geothermal resources in Nevada and the Great Basin. Geotherm. Res. Council Trans. 28, 13–18.

Coolbaugh, M., Zehner, R., Kreemer, C., Blackwell, D., Oppliger, G., Sawatzky, D., Blewitt, G., Pancha, A., Richards, M., Helm-Clark, C., Shevenell, L., Raines, G., Johnson, G., Minor, T., Boyd, T., 2005. Geothermal potential map of the Great Basin, western United States: Nevada. Bur. Mines Geol. Map (151).

Corti, G., Cuffaro, M., Doglioni, C., Innocenti, F., Manetti, P., 2006. Coexisting geodynamic processes in the Sicily channel. Geol. Soc. Am. 409, 83–96 (Special paper).

Cressie, N.A.C., 1991. Statistics for Spatial Data. John Wiley and Sons, Inc, New York, pp. 900.

Curewitz, D., Karson, J.A., 1997. Structural settings of hydrothermal outflow: fracture permeability maintained by fault propagation and interaction. J. Volcanol. Geotherm. Res. 79, 149–168.

D'Alessandro, W., Parello, F., Valenza, M., 1996. Gas manifestations of Mount Etna area: historical notices and new geochemical data (1990–1993). Acta Vulcanol. 8 (1), 23–29.

D'Alessandro, W., De Gregorio, S., Dongarrà, G., Guerrieri, S., Parello, F., Parisi, B., 1997. Chemical and isotopic characterization of the gases of Mount Etna (Italy). J. Volcanol. Geotherm. Res. 78, 65–76.
Davies, J.H., Davies, D.R., 2010. Earth surface heat flux. Solid Earth 1, 5–24.
De Gregorio, S., Diliberto, I.S., Giammanco, S., Gurrieri, S., Valenza, M., 2002. Tectonic control over large-scale diffuse degassing in eastern Sicily (Italy). Geofluids 2, 273–284.
Della Vedova, B., Bellani, S., Pellis, G., Squarci, P., 2001. Deep temperatures and surface heat flow distribution. In: Vai, G.B., Martini, I.P. (Eds.), Anatomy of an Orogen. The Apennines and Adjacent Mediterranean Basins. Kluwer Ac. Publ., Great Britain, pp. 65–76.
Deming, D., Chapman, D.S., 1988. Inversion of bottom-hole temperature data: the Pineview field, Utah–Wyoming thrust belt. Geophysics 53, 707–720.
Di Sipio, E., Chiesa, S., Destro, E., Galgaro, A., Giaretta, A., Gola, G., Manzella, A., 2013. Rock thermal conductivity as key parameter for geothermal numerical models. Energy Procedia 40 (2013), 87–94.
Doglioni, C., Ligi, M., Scrocca, D., Bigi, S., Bortoluzzi, G., Carminati, E., Cuffaro, M., D'Oriano, F., Forleo, V., Muccini, F., Riguzzi, F., 2012. The tectonic puzzle of the Messina area (Southern Italy): insights from new seismic reflection data. Sci. Rep. 2 (970), 1–9.
EBA Engineering Consultants Ltd., 2010. Geothermal Favourability Map - Northwest Territories - Report and geothermal map for Government of Northwest Territories (NWT) to advance understanding of the potential for geothermal energy production in the NWT. Environmental and Natural Resources, Saint-Lazare, Quebec, Canada.
ENEL, ENI-AGIP, CNR, ENEA, 1988. Inventario delle Risorse Geotermiche Nazionali—Indagine D'insieme Sul Territorio Nazionale. Ministero dell'Industria, del Commercio e dell'Artigianato (currently Ministero dello Sviluppo Economico), pp. 75.
Faulkner, D.R., Jackson, C.A.L., Lunn, R.J., Schlische, R.W., Shipton, Z.K., Wibberly, C.A.J., Withjack, M.O., 2010. A review of recent developments concerning the structure, mechanics and fluid flow properties of fault zones. J. Struct. Geol. 32 (11), 1557–1575.
Favara, R., Grassa, F., Inguaggiato, S., Valenza, M., 2001. Hydrogeochemistry and stable isotopes of thermal springs: earthquake-related chemical changes along Belice Fault (Western Sicily). Appl. Geochem. 16, 1–17.
Galgaro, A., Di Sipio, E., Destro, E., Chiesa, S., Uricchio, V.F., Bruno, D., Masciale, R., Lopez, N., Iaquinta, P., Teza, G., Iovine, G., Montanari, D., Manzella, A., Soleri, S., Greco, R., Di Bella, G., Monteleone, S., Sabatino, M., Iorio, M., Petruccione, E., Giaretta, A., Tranchida, G., Trumpy, E., Gola, G., D'arpa, S., 2012. Methodological approach for evaluating the geo-exchange potential: VIGOR Project. Acque Sotterr.: Ital. J. Groundw. 3 (130), 43–53.
Giammanco, S., Inguaggiato, S., Valenza, M., 1998. Soil and fumarole gases of Mount Etna: geochemistry and relations with volcanic activity. J. Volcanol. Geotherm. Res. 81, 297–310.
Giammanco, S., Palano, M., Scaltrito, A., Scarfì, L., Sortino, F., 2008. Possible role of fluid overpressure in the generation of earthquake swarms in active tectonic areas: the case of the Peloritani Mts. (Sicily, Italy). J. Volcanol. Geotherm. Res. 178, 795–806.
Giunta, G., 1985. Problematiche ed ipotesi sul bacino numidico nelle maghrebidi siciliane. Boll. Soc. Geol. It. 104, 239–256.
Grassa, F., (Ph.D. thesis) 2001. Geochemical Processes Governing The Chemistry Of Groundwater Hosted Within The Hyblean Acquifers (South-Eastern Sicily, Italy). University of Palermo, Italy.
Grassa, F., Capasso, G., Favara, R., Inguaggiato, S., 2006. Chemical and isotopic of waters and dissolved gases in some thermal springs of sicily and adjacent volcanic islands, Italy. Pure Appl. Geophys. 163, 781–807.
Gudmundsson, A., Berg, S.S., Lyslo, K.B., Skurtveit, E., 2001. Fracture networks and fluid transport in active fault zones. J. Struct. Geol. 23 (2–3), 343–353.
Haenel, R., Rybach, L., Stegena, L., 1988. Fundamentals of geothermics. In: Haenel, R., Rybach, L., Stegena (Eds.), Handbook of Terrestrial Heat Flow Density Determination, 1988. KJluwer Academic Publishers, Dordrecht, NL, pp. 9–57.
Hooker, P.J., Bertrami, R., Lombardi, S., O'Nions, R.K., Oxburgh, E.R., 1985. Helium-3 anomalies and crust–mantle interaction in Italy. Geochim. Cosmochim. Acta 49, 2505–2513.
Huenges, E., 2010. Geothermal Energy Systems–Exploration, Development and Utilization. Wiley-VCH, Weinheim, Germany, pp. 463.
IFC, 2013. Success of geothermal wells: a global study. Report by International Finance Corporation, on behalf of GeotherEx Inc., 80 pages, June 2013. ⟨www.ifc.org.⟩.
ISIDe Working Group INGV, 2010. Italian seismological instrumental and parametric database. ⟨http://iside.rm.ingv.it⟩ (accessed October 2013).
Jaeger, J.C., 1965. Application of the Theory Of Heat Conduction to Geothermal Measurements. In: Lee, W.H.K. (Ed.), Terrestrial Heat Flow. American Geophysical Union, Washington, D.C.
Katz, S.S., 1991. Emulating the PROSPECTOR expert system with a raster GIS. Computers & Geosciences 17, 1033–1050.
Keller, J., 1982. The Mediterranean island arcs. In: Thorpe, R.S. (Ed.), Andesites: Orogenic Andesites and Related Rocks. Wiley, Chichester, UK, pp. 307–332.
Kissling, Weir, 2005. The spatial distribution of geothermal fields in the Taupo Volcanic zone, New Zeland. J. Volcanol. Geotherm. Res. 145, 136–150.
Landolt-Börnstein, 1982. Numerical data and functional relationships in science and technology—new series, group v: geophysics and space research. In: Physical Properties of Rocks. Springer-Verlag, Berlin-Heidelberg-New York, pp. 373.
Madonia, P., Grassa, F., Cangemi, M., Musumeci, C., 2011. Geomorphological and geochemical characterization of the 11 August 2008 mud volcano eruption at S. Barbara village (Sicily Italy) and its possible relationship with seismic activity. Nat. Hazards Earth Syst. Sci. 11, 1545–1557.
Manzella, A., 2013. Geothermal development in southern Italy and the contribution of VIGOR Project. In: Proceeding of European Geothermal Congress 2013, June, Pisa.
Marty, B., Jambon, A., 1987. C/3He in volatile fluxes from the solid earth: implications for carbon geodynamics. Earth Planet. Sci. Lett. 83, 16–26.
Marty, B., Trull, T., Lussiez, P., Basile, I., Tanguy, J.C., 1994. He, Ar, O, Sr and Nd isotope constraints on the origin and evolution of Mount Etna magmatism. Earth Planet. Sci. Lett. 126, 23–39.
McPherson, B.J.O.L., Chapman, D.S., 1996. Thermal analysis of the southern Powder River Basin, Wyoming. Geophysics 61 (6), 1689–1701.
Minissale, A., 2004. Origin, transport and discharge of CO_2 in central Italy. Earth Sci. Rev. 66, 89–141.
Monaco, C., Mazzoli, S., Tortorici, L., 1996. Active thrust tectonics in western Sicily (southern Italy): the 1968 Belice earthquake sequence. Terra Nova 8, 372–381.
Monaco, C., De Guidi, G., 2006. Structural evidence for Neogene rotations in the eastern Sicilian fold and thrust belt. J. Struct. Geol. 28, 561–574.
Montanari, D., Bertini, G., Botteghi, S., Caielli, G., Caiozzi, F., Catalano, R., De Franco, R., Doveri, M., Gianelli, G., Gola, G., Manzella, A., Minissale, A., Montegrossi, G., Monteleone, S., Norini, G., Tranchida, G., Trumpy, E., 2013. Medium enthalpy geothermal systems in carbonate reservoirs, the Western Sicily example. In: Proceeding of European Geothermal Congress 2013, June, Pisa.
Montanari, D., Albanese, C., Catalano, R., Contino, A., Fedi, M., Gola, G., Iorio, M., La Manna, M., Monteleone, S., Trumpy, E., Valenti, V., Manzella, A., 2014. Contour map of the top of the regional geothermal reservoir of Sicily (Italy). Journal of Maps, doi: 10.1080/17445647.2014.935503.
Nigro, F., Renda, P., 1999. Evoluzione geologica ed assetto strutturale della Sicilia centro-settentrionale. Boll. Soc. Geol. Ital. 118, 375–388.
Noorollahi, Y., Itoi, R., Fujii, H., Tanaka, T., 2007. GIS model for geothermal resource exploration in Akita and Iwate prefectures northern Japan. Comput. Geosci. 33, 1008–1021.
Noorollahi, Y., Itoi, R., Fujii, H., Tanaka, T., 2008. GIS integration model for geothermal exploration and well siting. Geothermics 37, 107–131.
Norton, D., Knapp, R., 1997. Transport phenomena in hydrotermal systems: the nature of porosity. Am. J. Sci. 277, 913–936.
O'Nions, R.K., Oxburgh, E.R., 1988. Helium, volatile fluxes and the development of continental crust. Earth Planet. Sci. Lett. 90, 331–347.
Parello, F., Allard, P., D'Alessandro, W., Federico, C., Jean-Baptiste, P., Catani, O., 2000. Isotope geochemistry of Pantelleria volcanic fluids, Sicily Channel rift: a mantle volatile end-member for volcanism in southern Europe. Earth Planet. Sci. Lett. 180, 325–339.
Parello, F., D'Alessandro, W., Aiuppa, A., Federico, C., 2001. Cartografia Geochimica Degli Acquiferi Etnei. CNR Pubbl., Palermo, Italy, pp. 103 (N. 2190).
Parkhurst, D.L., Appelo, C.A.J., 1999. User's guide to PHREEQC (version 2): a computer program for speciation, batch-reaction, one-dimensional transport, and inverse geochemical calculations. U.S. Geological Survey Water-Resources Investigations Report 99-4259, pp.312.
Pasquale, V., Chiozzi, P., Gola, G., Verdoya, M., 2008. Depth–time correction of petroleum bottom-hole temperatures in the Po Plain, Italy. Geophysics 73, 187–196.
Pasquale, V., Gola, G., Chiozzi, P., Verdoya, M., 2011. Thermophysical properties of the Po Basin rocks. Geophys. J. Int. 186, 69–81.
Pasquale, V., Chiozzi, P., Verdoya, M., Gola, G., 2012. Heat flow in the Western Po Basin and surrounding orogenic belts. Geophys. J. Int. 190, 8–22.
Pasquale, V., Chiozzi, P., Verdoya, M., 2013. Evidence thermal convection in the deep carbonate aquifer of the eastern sector of the Po Plain, Italy. Tectonophysics 594, 1–12.
Patanè, D., Privitera, E., Gresta, S., Akinci, A., Alparone, S., Barberi, G., Chiaraluce, L., Cocina, O., D'Amico, S., De Gori, P., Di Grazia, G., Falsaperla, S., Ferrari, F., Gambino, S., Giampiccolo, E., Langer, H., Maiolino, V., Moretti, M., Mostaccio, A., Musumeci, C., Piccinini, D., Reitano, D., Scarfì, L., Spampinato, S., Ursino, A., Zuccarello, L., 2003. Seismological constraints for the dike emplacement of July–August 2001 lateral eruption at Mt. Etna volcano, Italy. Ann. Geophys. 46 (4), 599–608.
Pecoraino, G., Giammanco, S., 2005. Geochemical Characterization and Temporal Changes in Parietal Gas Emissions at Mt. Etna (Italy) During the Period July 2000 - July 2003. TAO, Vol. 16, No. 4, 805–841, October 2005.
Pollack, H.N., Hurter, S.J., Johnson, J.R., 1993. Heat flow from the Earth's interior: Analysis of the global data set. Rev. Geophys. 31 (3), 267–280, doi:10.1029/93RG01249.
Polyak, B.G., Prasolov, E.M., Buachidza, G.I., Kononov, V.I., Mamirin, B.A., Surovtseva, L.I., Khabarin, L.V., Yudenich, V.S., 1981. Isotopic distribution of helium and argon isotopes of fluids in the Alpine–Apennine region and its relationship to volcanism. Dokl. Akad. Nuak. SSSR 247, 1220–1225.
Prol-Ledesma, R.M., 2000. Evaluation of the reconnaissance results in geothermal exploration using GIS. Geothermics 29, 83–103.
Roure, F., Howell, D.G., Müller, C., Moretti, I., 1990. Late Cenozoic subduction complex of Sicily. J. Struct. Geol. 12, 259–266.
Saar, M.O., 2011. Review: Geothermal heat as a tracer of large-scale groundwater flow and as a means to determine permeability fields. Hydrogeol. J. 19, 31–52.
Sano, Y., Wakita, H., Italiano, F., Nuccio, P.M., 1989. Helium isotopes and tectonics in southern Italy. Geophys. Res. Lett. 16, 511–514.
Sanyal, S.K., 2005. Classification of geothermal systems–A possible scheme. In: Proceeding, Thirtheth Workshop on Geothermal Reservoir Engineering, Stanford University, Stanford, California, January 31–February 2, 2005, SGP-TR-176.

Sartori, R., 2003. The Tyrrhenian back-arc basin and subduction of the Ionian lithosphere. Episodes 26 (3), 217–221.
Sclater, J.G., Jaupart, C., Galson, D., 1980. The heat flow through oceanic and continental crust and the heat loss of the earth. Rev. Geophys. Space Phys. 18 (1), 269–311.
Shako, L., Mutua, J., 2011. Geo-scientific data integration to evaluate geothermal potential using GIS. In: Proceedings, Kenya Geothermal Conference, November, Nairobi.
Sibson, R.H., 1996. Structural permeability of fluid-driven fault-fracture meshes. J. Struct. Geol. 18 (8), 1031–1042.
Sibson, R.H., 1990. Conditions for fault-value behaviour. In: Knipe, R.J., Rutter, E.H. (Eds.), Deformation Mechanisms, Rheology and Tectonics., 54. Geological Society Special Publication, pp. 15–28.
Tassi, F., Capecchiacci, F., Cabassi, J., Calabrese, S., Vaselli, O., Rouwet, D., Pecoraino, G., Chiodini, G., 2012. Geogenic and atmospheric sources for volatile organic compounds in fumarolic emissions from Mt. Etna and Vulcano Island (Sicily, Italy). Journal of Geophysical Research 117, D17305, doi:10.1029/2012JD017642.
Tedesco, D., 1997. Systematic variations in the $^{3}He/^{4}He$ ratio and carbon of fumarolic fluids from active volcanic areas in Italy: evidence for radiogenic ^{4}He and crustal carbon addition by the subducting African plate? Earth Planet. Sci. Lett. 151, 255–269.
Tedesco, D., Allard, P., Sano, Y., Wakita, H., Pece, R., 1990. Helium-3 in subaerial and submarine fumaroles of Campi Flegrei caldera, Italy. Geochim. Cosmochim. Acta 54, 1105–1116.
Tufekci, N., Lutfi Suzen, M., Gulec, N., 2010. GIS based geothermal potential assessment: a case study from Western Anatolia, Turkey. Energy 35, 246–261.
Visini, F., de Nardis, R., Lavecchia, G., 2010. Rates of active compressional deformation in central Italy and Sicily: evaluation of the seismic budget. Int. J. Earth Sci. (Geol. Rundsch.) 99 (Suppl. 1), S243–S264.
Yousefi, H., Ehara, S., Noorollahi, Y., 2007. Geothermal potential site selection using GIS in Iran. Thirty-Second Workshop on Geothermal Reservoir Engineering, Stanford University, Stanford, California, January 22–24.
Yousefi, H., Noorollahi, Y., Ehara, S., Itoi, R., Yousefi, A., Fujimitsu, Y., Nishijima, J., Sasaki, K., 2010. Developing the geothermal map of Iran. Geotermics 39 (2), 140–151.